

TOPOLOGY PRESERVING 2-SUBFIELD 3D THINNING ALGORITHMS

Gábor Németh

Dept of Image Processing and Computer Graphics
University of Szeged
Szeged, Hungary
email: gnemeth@inf.u-szeged.hu

Péter Kardos and Kálmán Palágyi

Dept of Image Processing and Computer Graphics
University of Szeged
Szeged, Hungary
email: {pkardos, palagyi}@inf.u-szeged.hu

ABSTRACT

This paper presents a new family of 3D thinning algorithms for extracting skeleton-like shape features (i.e., centerline, medial surface, and topological kernel) from volumetric images. A 2-subfield strategy is applied: all points in a 3D picture are partitioned into two subsets which are alternatively activated. At each iteration, a parallel operator is applied for deleting some border points in the active subfield. The proposed algorithms are derived from Ma's sufficient conditions for topology preservation, and they use various endpoint characterizations.

KEY WORDS

Pattern recognition, Image representation, Shape analysis, 3D data analysis, Skeleton, Thinning algorithms.

1 Introduction

Skeletons are shape descriptors which show the essential topology and summarize the general form of objects in binary images [2]. They have been studied for over forty years in image processing, pattern recognition, and visualization. Extracting skeleton-like shape descriptors from 3D binary objects is useful in numerous applications, such as topological analysis [3], measurement [15], surface generation [5], shape deformation [20], shape matching [18], or automatic navigation [6, 21].

A 3D binary picture [8] is a mapping that assigns a value of 0 or 1 to each point with integer coordinates in the 3D digital space denoted by \mathbb{Z}^3 , where points having the value of 1 (i.e., *black* points) form the objects of a picture and points with a 0 value (i.e., *white* points) compose the background and the cavities of a picture. A *parallel reduction operation* changes some black points to white ones (which is referred to as *deletion*) simultaneously. A parallel reduction operator does not *preserve topology* [7] if any object in the input picture is split or is completely deleted, any cavity/hole in the input picture is merged with the background or another cavity/hole, or a cavity/hole is created where there was none in the input picture.

Parallel thinning algorithms [4] are frequently applied for extracting "skeletons" in a topology preserving way [8]. They use parallel reduction operations: some black border points of a binary object that satisfy certain topological and geometric constraints are deleted simultane-

ously at an iteration step, and the entire process is repeated until stability is achieved.

Thinning algorithms delete black points which are not *endpoints*, since preserving endpoints provides important geometrical information relative to the shape of the objects. In 3D [1], there are three kinds of skeleton-like shape features: surface-thinning algorithms extract *medial surfaces* by preserving *surface-endpoints*, curve-thinning algorithms produce *centerlines* by preserving *curve-endpoints*, and *topological kernels* (i.e., minimal structures which are topologically equivalent to the original objects) can be generated if no endpoint criteria are considered during the iterative object reduction.

One kind of parallel thinning approach is the *subfield-based* method [4]. In subfield-based 3D thinning algorithms, the digital space \mathbb{Z}^3 is partitioned into more subsets which are alternatively activated. At a given iteration step, only black points in the active subfield can be designated to be deleted.

Existing subfield-based parallel thinning algorithms working on the cubic grid \mathbb{Z}^3 use two [10, 11, 13], four [12], and eight [1, 16] subfields. Their deletion rules are rather complicated, and their topological correctness need complex proofs.

In this paper, we propose a new family of parallel 2-subfield 3D thinning algorithms that are based on Ma's sufficient conditions for parallel reduction operators [9]. Hence their topological correctness is self-evident. Our algorithms differ from each other in the considered endpoint characterizations. They are computationally efficient due to the applied implementation method.

2 Basic Notions

Let p be a point in the 3D digital space \mathbb{Z}^3 . Let us denote $N_j(p)$ (for $j = 6, 18, 26$) the set of points that are j -adjacent to p (see Figure 1a).

The sequence of distinct points $\langle x_0, x_1, \dots, x_n \rangle$ is called a j -path (for $j = 6, 18, 26$) of length n from point x_0 to point x_n in a non-empty set of points X if each point of the sequence is in X and x_i is j -adjacent to x_{i-1} for each $1 \leq i \leq n$. Note that a single point is a j -path of length 0. Two points are said to be j -connected in the set X if there is a j -path in X between them.

The 3D binary $(26, 6)$ digital picture \mathcal{P} is a quadru-

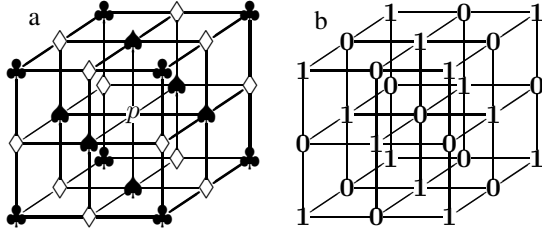


Figure 1. Frequently used adjacencies in \mathbb{Z}^3 (a) and partitioning of \mathbb{Z}^3 into two subfields (b).

The set $N_6(p)$ contains point p and the 6 points marked “♠”. The set $N_{18}(p)$ contains $N_6(p)$ and the 12 points marked “◇”. The set $N_{26}(p)$ contains $N_{18}(p)$ and the 8 points marked “♣”.

The division of \mathbb{Z}^3 into two subfields S_0 and S_1 forms a “chessboard-like” partitioning, where points marked “ i ” are in subfield S_i ($i = 0, 1$).

ple $\mathcal{P} = (\mathbb{Z}^3, 26, 6, B)$ [8]. Each point in $B \subseteq \mathbb{Z}^3$ is called a *black point* and has a value of 1 assigned to it. Each point in $\mathbb{Z}^3 \setminus B$ is called a *white point* and has a value of 0. 26-adjacency is associated with the black points, and 6-adjacency is assigned to the white points. A *black component* is a maximal 26-connected set of points in B , while a *white component* is a maximal 6-connected set of points in $\mathbb{Z}^3 \setminus B$. Here it is assumed that a picture contains finitely many black points.

A black point is called a *border point* in $(26, 6)$ pictures if it is 6-adjacent to at least one white point. A black point is called an *interior point* if it is not a border point. A black point is called an *isolated point* if it is not 26-adjacent to any other black point. A *simple point* is a black point whose deletion is a topology preserving reduction [8]. Note that interior and isolated points are not simple, and the simplicity of a point p can be decided by examining the set $N_{26}(p)$.

Parallel reduction operators delete a set of black points and not just a single simple point. Next, we need to consider what is meant by topology preservation when a number of black points are deleted simultaneously.

Definition 1 [9] Let P be a $(26, 6)$ picture. The set of black points $D = \{d_1, \dots, d_k\}$ is called a simple set of P if D can be arranged in a sequence $\langle d_{i_1}, \dots, d_{i_k} \rangle$ in which d_{i_1} is simple and each d_{i_j} is simple after $\{d_{i_1}, \dots, d_{i_{j-1}}\}$ is deleted from P , for $j = 2, \dots, k$. (By definition, let the empty set be simple.)

Theorem 1 [9] A 3D parallel reduction operation preserves topology for $(26, 6)$ pictures if all of the following conditions hold:

1. Only simple points can be deleted.
2. If two, three, or four elements of a 2×2 square are deleted, then these points form a simple set.

3. No black component contained in a $2 \times 2 \times 2$ cube in \mathbb{Z}^3 can be deleted completely.

In 2-subfield 3D thinning algorithms, the cubic grid \mathbb{Z}^3 is partitioned into two subsets S_0 and S_1 , where

$$S_0 = \{ (p_x, p_y, p_z) \in \mathbb{Z}^3 \mid p_x + p_y + p_z \equiv 0 \pmod{2} \},$$

$$S_1 = \{ (p_x, p_y, p_z) \in \mathbb{Z}^3 \mid p_x + p_y + p_z \equiv 1 \pmod{2} \}.$$

We can state that two points p and $q \in N_{26}(p)$ are both in the same subfield if $q \in N_{18}(p) \setminus N_6(p)$ (see Figure 1b). Consequently, Ma’s sufficient conditions for topology preservation (see Theorem 1) can be simplified for 3D parallel reduction operations working on two subfields as follows:

Theorem 2 [12] A 2-subfield 3D parallel reduction operation preserves topology for $(26, 6)$ pictures if all of the following conditions hold:

1. Only simple points can be deleted.
2. If two points p and $q \in N_{18}(p) \setminus N_6(p)$ are deleted, then $\{p, q\}$ is a simple set.
3. No black component of two, three, or four mutually 18-adjacent, but not 6-adjacent points can be deleted completely.

Our new 2-subfield 3D thinning algorithms are based on Theorem 2 by using various endpoint characterizations.

3 The New Family of 2-Subfield Thinning Algorithms

In this section, a family of 2-subfield 3D thinning algorithms are presented for extracting skeleton-like shape features. Our algorithms are derived from Ma’s simplified conditions (see Theorem 2). Let us lay down their deletable points:

Definition 2 Let us consider an arbitrary characterization of endpoints that is called as type \mathcal{T} . A black point in a $(26, 6)$ picture \mathcal{P} is self- \mathcal{T} -deletable if it is not an endpoint of type \mathcal{T} and it is simple in \mathcal{P} .

Definition 3 Black point p in a $(26, 6)$ picture \mathcal{P} is square- \mathcal{T} -deletable if p is self- \mathcal{T} -deletable (see Definition 2), and for any self- \mathcal{T} -deletable point $q \in N_{18}(p) \setminus N_6(p)$, the set $\{p, q\}$ is simple in \mathcal{P} .

Definition 4 A black point in a $(26, 6)$ picture is cube- \mathcal{T} -deletable if it does not come first in the lexicographic ordering of black components of square- \mathcal{T} -deletable points depicted in Figure 2.

We are now ready to define the \mathcal{T} -deletable points.

Definition 5 Black point p in a $(26, 6)$ picture \mathcal{P} is \mathcal{T} -deletable if p is self- \mathcal{T} -deletable (see Definition 2), square- \mathcal{T} -deletable (see Definition 3), and cube- \mathcal{T} -deletable (see Definition 4).

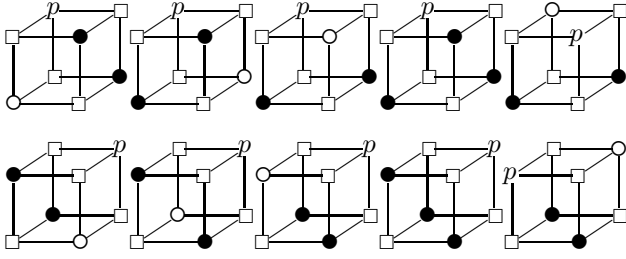


Figure 2. Black components of mutually 18-adjacent, but not 6-adjacent points in which square- \mathcal{T} -deletable point p is not cube- \mathcal{T} -deletable. Notations: each point marked “●” is a square- \mathcal{T} -deletable black point; each point marked “○” is a white point; each point marked “□” is a white point. (Note that all points marked “○” and p are in the same subfield, and any point marked “□” and p are in different subfields.)

Note that various characterizations of endpoints yield different types of deletable points. By Definition 5, we introduce the following 2-subfield thinning algorithm that preserves endpoints of type \mathcal{T} :

Algorithm- \mathcal{T}

Input: picture $(\mathbb{Z}^3, 26, 6, X)$
Output: picture $(\mathbb{Z}^3, 26, 6, Y)$
 $Y = X$
repeat
 // one iteration step
 // phase 1 – subfield S_0 is active
 $D_0 = \{ p \mid p \text{ is } \mathcal{T}\text{-deletable in } Y \cap S_0 \}$
 $Y = Y \setminus D_0$
 // phase 2 – subfield S_1 is active
 $D_1 = \{ p \mid p \text{ is } \mathcal{T}\text{-deletable in } Y \cap S_1 \}$
 $Y = Y \setminus D_1$
until $D_0 \cup D_1 = \emptyset$

Various characterizations of endpoints yield different algorithms. We can prove the topological correctness of the proposed algorithms:

Theorem 3 *Algorithm- \mathcal{T} preserves topology for $(26,6)$ pictures.*

Proof. To prove it, we show that parallel reductions of the proposed algorithms (i.e., deletions of the sets of \mathcal{T} -deletable points, see Definition 5) satisfy all conditions of Theorem 2.

1. \mathcal{T} -deletable points are self- \mathcal{T} -deletable ones (see Definitions 2 and 5) and self- \mathcal{T} -deletable points are simple points (see Definition 2), hence their deletion satisfies Condition 1 of Theorem 2.

2. \mathcal{T} -deletable points are square- \mathcal{T} -deletable ones (see Definitions 3 and 5). It can be readily seen that deletion of square- \mathcal{T} -deletable points (see Definition 3), satisfies Condition 2 of Theorem 2.

3. Let us consider black components of two, three, or four mutually 18-adjacent, but not 6-adjacent \mathcal{T} -deletable points.

- Let $C = \{p, q\}$ be such a black component of two points. It is easy to see, that p is an isolated point after the deletion of q , and q is an isolated point after the deletion of p . An isolated point is not simple, hence, $\{p, q\}$ is not a simple set. Therefore, p and q are not square- \mathcal{T} -deletable points (see Definition 3). Thus, they are not \mathcal{T} -deletable points (see Definition 5). Hence, C cannot be deleted completely, thus Condition 3 of Theorem 2 holds for black components of two elements.
- Next we need to consider black components of three or four mutually 18-adjacent, but not 6-adjacent points.

It can be readily seen that all the possible ten cases are depicted in Figure 2. In each black component, black point p is not cube- \mathcal{T} -deletable (see Definition 4), hence, p is not \mathcal{T} -deletable (see Definition 5). Since p cannot be deleted, the considered component cannot be deleted completely. Thus, Condition 3 of Theorem 2 holds.

4 Examples of the Proposed Algorithms

In the previous section, a general algorithm is presented that preserves endpoints of type \mathcal{T} , where \mathcal{T} is an arbitrary characterization of curve-endpoints or surface-endpoints. Here, we present six kinds of 2-subfield 3D thinning algorithms according to the following types of endpoints:

Definition 6 *Any black point in a $(26,6)$ picture is not an endpoint of type TK. (If no endpoints are preserved during the thinning process, then we get topological kernels.)*

Definition 7 [1] *Black point p in picture $(\mathbb{Z}^3, 26, 6, B)$ is a curve-endpoint of type C1 if the set $(N_{26}(p) \setminus \{p\}) \cap B$ contains at least two black components.*

Definition 8 *Black point p in picture $(\mathbb{Z}^3, 26, 6, B)$ is a curve-endpoint of type C2 if $(N_{26}(p) \setminus \{p\}) \cap B = \{q\}$*

- $(N_{26}(q) \setminus \{q\}) \cap B = \{p\}$ or
- $(N_{26}(q) \setminus \{q\}) \cap B = \{p, r\}$.

Definition 9 *Black point p in picture $(\mathbb{Z}^3, 26, 6, B)$ is a curve-endpoint of type C3 if $(N_{26}(p) \setminus \{p\}) \cap B = \{q\}$ and*

- $(N_{26}(q) \setminus \{q\}) \cap B = \{p\}$ or

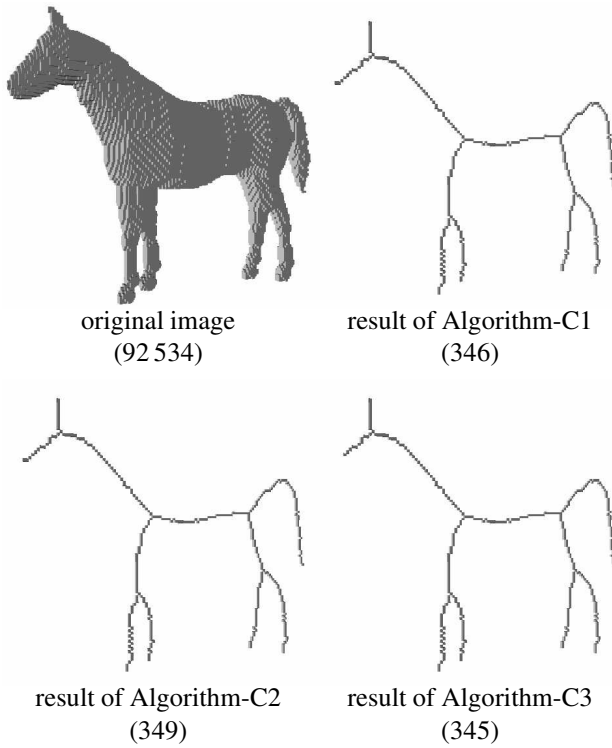


Figure 3. A $140 \times 140 \times 50$ image of a horse and its “skeletons” produced by our algorithms.

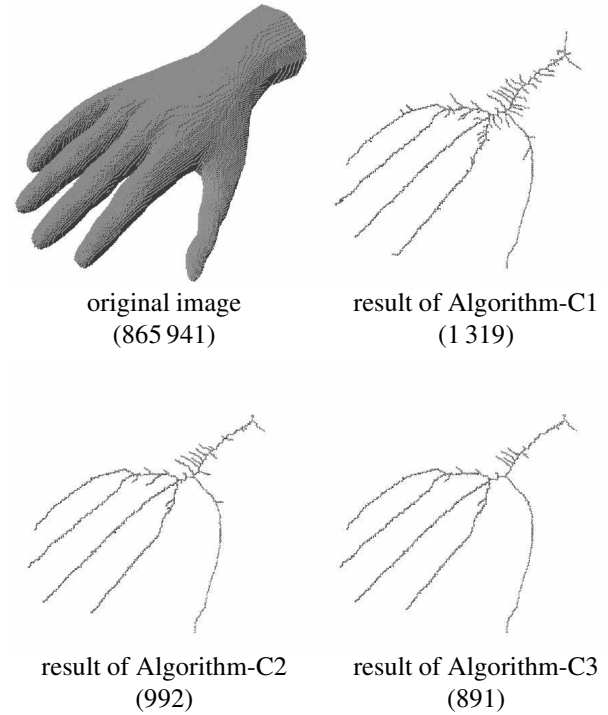


Figure 4. A $174 \times 103 \times 300$ image of a hand and its “skeletons” produced by our algorithms.

- $(N_{26}(q) \setminus \{q\}) \cap B = \{p, r\}$ and point r is 26-adjacent to at most two black points.

Note that characterizations of curve-endpoints according to Definitions 8 and 9 were inspired by the concept “twig voxel” that was introduced by Ma, Wan, and Chang [11].

Definition 10 [1] Black point p in picture $(\mathbb{Z}^3, 26, 6, B)$ is a surface-endpoint of type S1 if p is a curve-endpoint of type C1 (see Definition 7) or the set $N_{26}(p) \cap (\mathbb{Z}^3 \setminus B)$ contains at least two white components.

Definition 11 [14] Black point p in picture $(\mathbb{Z}^3, 26, 6, B)$ is a surface-endpoint of type S2 if there is no interior point in the set $N_6(p) \cap B$.

In experiments these six 2-subfield 3D thinning algorithms were tested on objects of different shapes. Here we present some illustrative examples below (Figures 3-8). Numbers in parentheses mean the count of black points.

It is well-known, that 3D skeletons generally contain surface patches (i.e., branched 2D manifolds). In the case of tubular objects, we need a skeletonization method that can suppress creation of such surface segments. As a solution, curve-thinning (i.e., iterative object reduction that preserves curve-endpoints) is proposed. The first three test objects (see Figures 3-5) are tubular, hence their centerlines are extracted by three of the proposed curve-thinning algorithms.

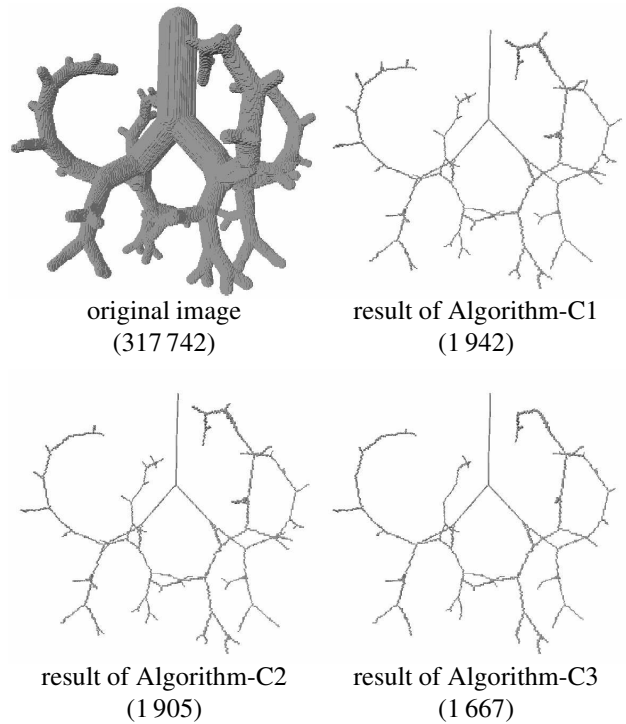


Figure 5. A $300 \times 300 \times 300$ image of a tubular structure and its “skeletons” produced by our algorithms.

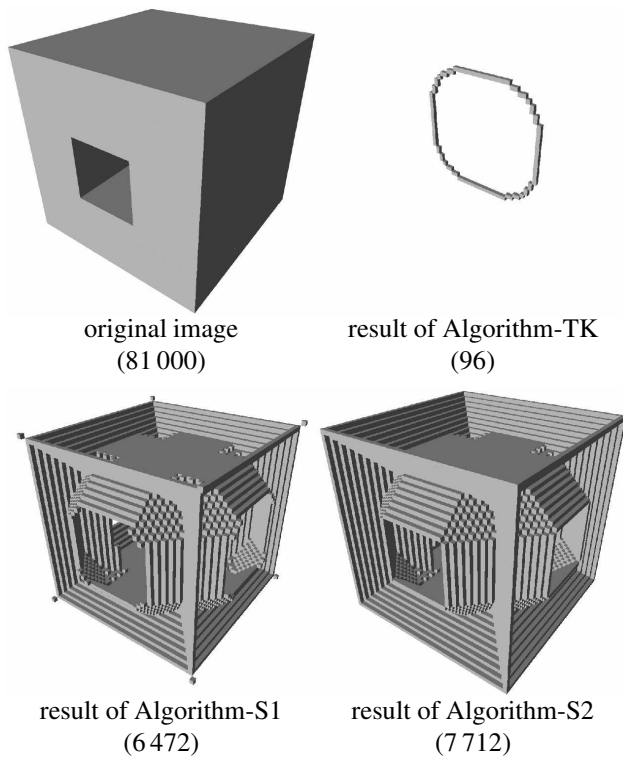


Figure 6. The 3D image of a $45 \times 45 \times 45$ cube with a hole and its “skeletons” produced by our algorithms.

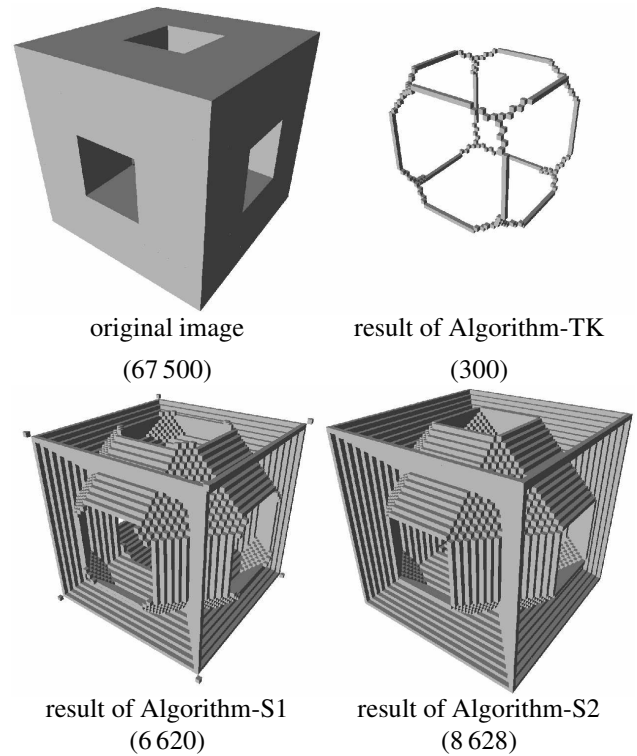


Figure 8. The 3D image of a $45 \times 45 \times 45$ cube with three holes and its “skeletons” produced by our algorithms.

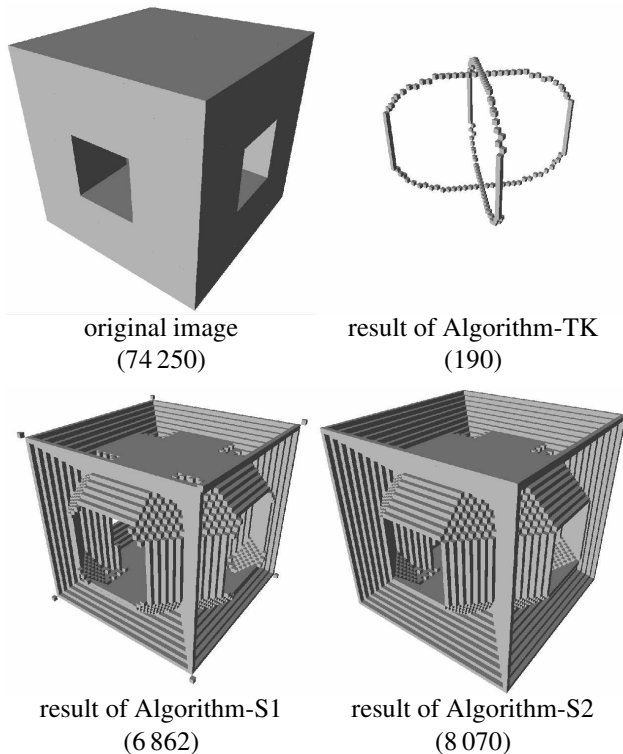


Figure 7. The 3D image of a $45 \times 45 \times 45$ cube with two holes and its “skeletons” produced by our algorithms.







Note that the first three test objects contain neither holes nor cavities, hence Algorithm-TK (i.e., the algorithm for extracting topological kernels, see Definition 6) produces only one isolated point for such an object. Isolated points produced by Algorithm-TK are not depicted in Figures 3-5. Topological kernels of the remaining three test objects (see Figures 6-8) are much more sightly. They are formed by 1-point thick closed curves, since the original objects contain some holes.

On the one hand, skeletons are sensitive to coarse object boundaries; on the other hand, some endpoints may be generated by the iterative thinning process. As a result, the “skeleton” produced generally includes false segments that must be removed by a pruning step [15, 17, 19]. Let us see Figure 4. We can state that Algorithm-C1 produces relative large number of false side branches, since the other two algorithms (that use the more sophisticated types of curve-endpoints C2 and C3) generate much fewer undesired segments to be pruned.

Some medial surfaces generated by Algorithm-S1 and Algorithm-S2 are depicted in Figures 6-8. We can state that Algorithm-S2 seems to be better than Algorithm-S1. It can produce more compact “skeletons” without overshrinking the original objects.

A critic, however, might think that the proposed algorithms are time consuming and it is rather difficult to implement them on standard sequential computers. Thus we sketch here an efficient and fairly general implementation

Table 1. Computation times for the given six kinds of test objects (see Figures 3-8). The implemented algorithms were run under Linux on an Intel Pentium 4 CPU 2.80 GHz PC.

Test object	Type of endpoints	Comp. time (sec.)
	C1	0.18
	C2	0.18
	C3	0.18
	C1	1.75
	C2	1.74
	C3	1.75
	C1	1.33
	C2	1.34
	C3	1.17
	TK	0.11
	S1	0.09
	S2	0.11
	TK	0.09
	S1	0.08
	S2	0.11
	TK	0.09
	S1	0.08
	S2	0.09

method [14].

The proposed implementation uses a pre-calculated look-up-table to encode the simple points. Since the simplicity of a point p in a $(26,6)$ picture can be decided by examining the set $N_{26}(p)$, that table has 2^{26} entries of 1 bit in size, hence it requires just 8 MB of storage space in memory.

In addition, two lists are used to speed up the process: one for storing the border points in the current picture (since thinning can only delete border-points, thus the repeated scans of the entire array storing the picture are not needed); the second list is to store all deletable points in the current phase of the process. At each iteration, the deletable points are deleted, and the list of border points is updated accordingly.

The proposed method makes possible a computationally efficient implementation. Its efficiency is illustrated in Table 1.

5 Conclusion

Fast skeleton extraction is extremely important in numerous applications for large 3D shapes. In this paper, we presented a new family of 2-subfield 3D thinning algorithms that are based on Ma's sufficient conditions for topology preservation. Hence, the topological correctness of our algorithms is self-evident. Six variations for the proposed

thinning scheme were presented by considering six different types of endpoint characterizations. Thanks to the efficient implementation, our algorithms are very fast. The proposed method is capable of extracting three kinds of skeleton-like shape features (i.e., medial surface, centerline, and topological kernel) according to the applied endpoint characterization. Medial surfaces are generally extracted from general shapes, tubular structures can be represented by their centerlines, and topological kernels are fairly useful in topological description. Skeletonization is sensitive to coarse object boundaries, hence a thinning process is to be coupled with an efficient pruning method.

Acknowledgements

This research was partially supported by the TÁMOP-4.2.2/08/1/2008-0008 program of the Hungarian National Development Agency.

The authors would like to thank Stina Svensson (Swedish University of Agricultural Sciences, Uppsala, Sweden), Nicu D. Cornea (The State University of New Jersey, USA), and Milan Sonka (The University of Iowa, USA) for supplying the data sets for Figures 3-5.

References

- [1] G. Bertrand, Z. Aktouf, A 3D thinning algorithm using subfields, *SPIE Proc. of Conf. on Vision Geometry*, San Diego, CA, USA, 1994, 113–124.
- [2] H. Blum, A transformation for extracting new descriptors of shape, *Models for the Perception of Speech and Visual Form*, (MIT Press, 1967) 362–380.
- [3] B.R. Gomberg, P.K. Saha, H.K. Song, S.N. Hwang, F.W. Wehrli, Topological analysis of trabecular bone MR images, *IEEE Transactions on Medical Imaging*, 19(3), 2000, 166–174.
- [4] R.W. Hall, Parallel connectivity-preserving thinning algorithms, in T.Y. Kong, A. Rosenfeld (Eds.) *Topological algorithms for digital image processing*, (Elsevier Science, 1996) 145–179.
- [5] T. Itoh, Y. Yamaguchi, K. Koyamada, Fast isosurface generation using the volume thinning algorithm, *IEEE Transactions on Visualization and Computer Graphics*, 7(1), 2001, 32–46.
- [6] A.P. Kiraly, J.P. Helferty, E.A. Hoffman, G. McLennan, W.E. Higgins, Three-dimensional path planning for virtual bronchoscopy, *IEEE Transaction on Medical Imaging*, 23(11), 2004, 1365–1379.
- [7] T.Y. Kong, On topology preservation in 2-d and 3-d thinning. *International Journal of Pattern Recognition and Artificial Intelligence*, 9, 1995, 813–844.

- [8] T.Y. Kong, A. Rosenfeld, Digital topology: Introduction and survey. *Computer Vision, Graphics, and Image Processing*, 48, 1989, 357–393.
- [9] C.M. Ma, On topology preservation in 3D thinning, *CVGIP: Image Understanding*, 59, 1994, 328–339.
- [10] C.M. Ma, S.Y. Wan, A medial-surface oriented 3-d two-subfield thinning algorithm, *Pattern Recognition Letters*, 22(13), 2001, 1439–1446.
- [11] C.M. Ma, S.Y. Wan, H.K. Chang, Extracting medial curves on 3D images, *Pattern Recognition Letters*, 23(8), 2002, 895–904.
- [12] C.M. Ma, S.Y. Wan, J.D. Lee, Three-dimensional topology preserving reduction on the 4-subfields, *IEEE Transaction on Pattern Analysis and Machine Intelligence*, 24(12), 2002, 1594–1605.
- [13] K. Palágyi, A 2-subfield 3D thinning algorithm for extracting medial curves, *Proc. Joint Hungarian-Austrian Conference on Image Processing and Pattern Recognition HACIPPR 2005*, Austrian Computer Society, 2005, 135–142.
- [14] K. Palágyi, A 3D fully parallel surface-thinning algorithm, *Theoretical Computer Science*, 406(1-2), 2008, 119–135.
- [15] K. Palágyi, J. Tschirren, E.A. Hoffman, M. Sonka, Quantitative analysis of pulmonary airway tree structures, *Computers in Biology and Medicine*, 36, 2006, 974–996.
- [16] P.K. Saha, B.B. Chaudhuri, D. Dutta Majumder, A new shape preserving parallel thinning algorithm for 3D digital images, *Pattern Recognition*, 19(12), 1998, 1119–1124.
- [17] D. Shaked, A. Bruckstein, Pruning medial axes, *Computer Vision and Image Understanding*, 69, 1998, 156–169.
- [18] H. Sundar, D. Silver, N. Gagvani, S. Dickinson, Skeleton based shape matching and retrieval, *Proc. Shape Modeling International*, 2003, 130–139.
- [19] S. Svensson, G. Sanniti di Baja, Simplifying curve skeletons in volume images, *Computer Vision and Image Understanding*, 90, 2003, 242–257.
- [20] H.B. Yan, S.M. Hu, R.R. Martin, Y.L. Yang, Shape deformation using a skeleton to drive simplex transformations, *IEEE Transactions on Visualization and Computer Graphics*, 14(3), 2008, 693–706.
- [21] M. Wan, Z. Liang, Q. Ke, L. Hong, I. Bitter, A. Kaufman, Automatic centerline extraction for virtual colonoscopy, *IEEE Transactions on Medical Imaging*, 21(12), 2002, 1450–1460.